Journal of Thermal Analysis, Vol. 47 (1996) 1407-1418

A MODULATED DIFFERENTIAL SCANNING CALORIMETRIC STUDY
Glass transitions occurring in sucrose solutions

M. J. Izzard, S. Ablett, P. J. Lillford, V. L. Hill[1] and I. F. Groves[1]*

Unilever Research, Colworth House, Sharnbrook, Bedfordshire, MK44 1LQ
[1]TA Instruments Ltd., Europe House, Bilton Centre, Cleeve Road, Leatherhead, Surrey, KT22 7UQ, England

Abstract

Modulated Differential Scanning Calorimetry™ has been applied to frozen sucrose solutions in the concentration range 10–80% w/w. The results from this study present, for the first time, information on the reversing and non-reversing nature of events that occur in these solutions. The study demonstrates the potential benefits of this new technique to help separate complex transitions that can occur in the total heat-flow curves obtained using traditional differential scanning calorimetry.

The results illustrate how this new technique can separate the different enthalpic events, which relate to the glass transition and the onset of ice dissolution that occurs during the heating of these frozen systems, by nature of their "reversing" and "non-reversing" contributions to the total heat flow.

Keywords: enthalpic relaxation, glass transition, modulated differential scanning calorimetry, non-reversing heat flow, reversing heat flow, sucrose solutions

Introduction

It is now well established [1–7] that the glass transition is an important physicochemical event in relation to food-product properties. This alternative approach [3–5] to the understanding of the properties of food materials means that there is currently much interest in how the glass transition temperature (T_g) can be measured [8]. The most widely applied technique is differential scanning calorimetry [3, 7, 9–11] (DSC), but the application of this technique has caused some controversy in terms of how the curves are to be interpreted, particularly for those obtained from freeze-concentrated samples [12–17]. The curves ob-

* Author to whom all correspondence should be addressed.

0368–4466/96/ $ 5.00

John Wiley & Sons, Limited
Chichester

tained from frozen materials are particularly complicated, due to different thermal events occurring over a very limited temperature range, i.e. the glass transition, an enthalpic relaxation process, and the onset of ice dissolution can all occur within a temperature range of a few degrees centigrade.

Modulated Differential Scanning Calorimetry (MDSC) is a new technique that has several advantages over the normal DSC technique [18–25]. The most significant of these is its ability to differentiate between different types of thermal events [26]. The MDSC mode of operation is an enhancement to the normal DSC, which allows it to provide extra information from a single experiment [26]. As well as providing the traditional DSC heat-flow and temperature information, MDSC provides information about the reversing and non-reversing characteristics of thermal events. This may aid the interpretation of the origin of the thermal behaviour of materials [27, 28]. The thermal events that take place in frozen systems have been most widely studied by DSC on frozen sucrose solutions [12–15, 17], hence this was chosen as a model system to be used in the evaluation of the applicability of MDSC to frozen food materials.

Materials and methods

Preparation of sucrose solutions

Sucrose (analytical-reagent grade) and purified water were obtained from BDH (Poole). Solutions were prepared by gently warming a weighed dispersion, as previously described [12]. The concentration of sucrose solutions in the range 10–80% w/w was confirmed by refractive index measurements made with an Abbe refractometer. Refractometer measurements were carried out immediately prior to MDSC measurements, and sucrose concentrations were determined according to previously described procedures [12]. In each case, the correct operation of the refractometer was confirmed by analysing purified water. Samples were stored in a domestic freezer at approximately –20°C and allowed to warm to room temperature before use; no solute crystallisation was observed after storage for periods of up to six months.

Instrumentation

Samples were analyzed using a TA Instruments DSC 2920 equipped with a cooling accessory and MDSC capability. A Liquid Nitrogen Cooling Accessory (LNCA) was used for the analysis of unannealed samples. This system permits a starting temperature of –150°C. A Refrigerated Cooling System (RCS) was used to anneal samples at –40°C and for the analysis of these annealed samples. The RCS is a self-contained refrigeration unit with an operating range of –70°C to 400°C. The DSC cell was purged with dry nitrogen gas flowing at 20 cm^3 min^{-1}.

The RCS was purged with nitrogen or helium gas flowing at 100 cm^3 min^{-1}, as required.

DSC calibration

Temperature calibration was carried out at a ramp rate of 2 °C min^{-1} using GPR-grade *n*-octane and *n*-decane (BDH, Poole), cyclohexane (Riedel-de Haën, 99.9%) and indium (Goodfellows Metals, 99.999%), which have melting points of –56.8, –26.66, 6.54 and 156.61 °C, respectively. The calorimetric response was calibrated against the known melting enthalpy of indium [29]. Enthalpic energies (J g^{-1} of sample) were determined by peak integration from the onset to the end of the enthalpic event. The change in heat capacity (ΔC_p) occurring at the glass transition was calculated in J g^{-1} °C^{-1} of sample.

DSC sample preparation

All samples were run in hermetically sealed aluminium pans. The lids of these pans were flattened to improve thermal contact with the sample. The empty sample and reference pans were matched by weight to within 0.15 mg for all experiments. The reference pan contained only air. All pans and sucrose solutions were weighed using a 5-figure Sartorius balance, type RC 210D. The balance was calibrated each morning before use, using an internal calibration procedure. Sucrose solution weights between 7.36 and 14.36 mg were used.

Temperature programme

Unannealed samples were prepared by cooling to –100 °C at approximately 50 °C min^{-1}, using the LNCA, and then heating at an underlying rate of 2 °C min^{-1}, amplitude ± 0.3 °C and period of 60 s. Annealed sucrose solutions were held at –40 °C for 1000 min, after initially cooling to –100 °C min^{-1}, to allow maximum ice devitrification to take place. At the end of this period, the sample was rapidly cooled to –70 °C and then heated in MDSC mode, using an underlying heating rate of 2 °C min^{-1} from –70 °C to 20 °C, with a temperature modulation of ±0.3 °C and a period of 60 s.

Modulated DSC

In the MDSC technique, a sinusoidal oscillation is overlaid on the conventional, linear temperature ramp or isotherm. The oscillation is characterised in terms of the period and amplitude of temperature modulation, which occurs for the underlying heating rate as shown in Fig. 1. Each of these three parameters can be varied independently. If the temperature oscillation is set with a large amplitude and short period, it is possible to obtain relatively high instantaneous

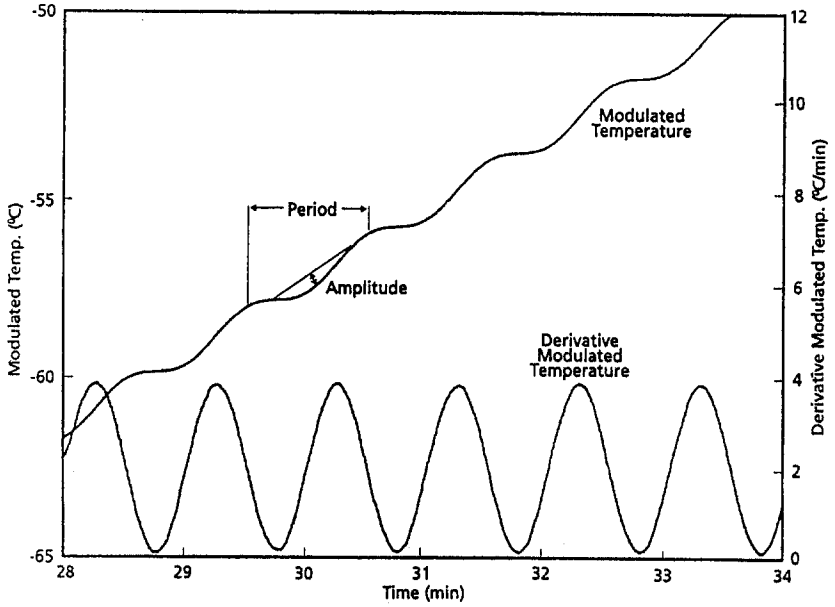

Fig. 1 DSC curve showing the modulated temperature programme and the derivative of this signal

heating rates during each oscillation cycle, even when the underlying heating rate is comparatively low. This maximises sensitivity without loss of resolution. The modulated temperature programme results in a modulated heat-flow signal that is deconvoluted in real time, using a simple Fourier transformation algorithm, into reversing, non-reversing and heat-capacity signals.

The modulated heat-flow signal can be expressed mathematically as:

$$\frac{dQ}{dt} = \frac{dT}{dt}(C_p + f_R(t,T)) + f_A(t,T)$$

where dQ/dt= heat flow; dT/dt=heating rate; C_p=sample heat capacity; t=time; T=temperature; $f_R(t,T)$ and $f_A(t,T)$=functions of time and temperature, which govern the kinetic response of any physical or chemical transition observed in DSC.

The DSC heat flow is seen to comprise two components, one that depends on heating rate ($C_p+f_R(t,T)$) and one that depends only on absolute temperature ($f_A(t,T)$).

The deconvolution process separates these two components, which are designated "reversing" and "non-reversing", respectively. MDSC also measures the total DSC heat-flow signal (average heat-flow amplitude), which gives information identical to that obtained from a conventional DSC experiment at the same underlying heating rate. The separation of these two heat-flow compo-

nents can aid in the interpretation of complex transitions by separating different types of thermal processes. For example, the change in heat capacity at a glass transition can be separated from an associated stress-relaxation endotherm [26]. The glass transition, due to its dependence on heating rate and time (i.e frequency), will be seen in the reversing heat-flow signal, whereas the stress-relaxation endotherm, which is dependent only on absolute temperature, will be seen in the non-reversing heat-flow signal.

Figure 2 shows the type of data produced directly from MDSC for a 65% w/w sucrose solution. The heat-flow signal is seen to be modulated in response to the modulated heating rate. The heat-flow can be seen to vary in two ways during a transition. There is a change in the amplitude of the modulation and/or in the underlying heat-flow value. This difference in response allows the total heat-flow to be resolved into reversing (a change in amplitude) and non-reversing (a change in underlying value) heat-flow components. The separation of these types of heat-flow aids in the interpretation of complex transitions.

It should also be noted that when the total, reversing, and non-reversing heat-flow traces are plotted on the same curve, they are scaled to the same heat-flow units (W/g of sample) in that curve. All the curves have been normalised, in order to take into account variations in initial sample weight. The initial values of the heat-flow traces have no special significance; they merely assist in the presentation of the experimental data.

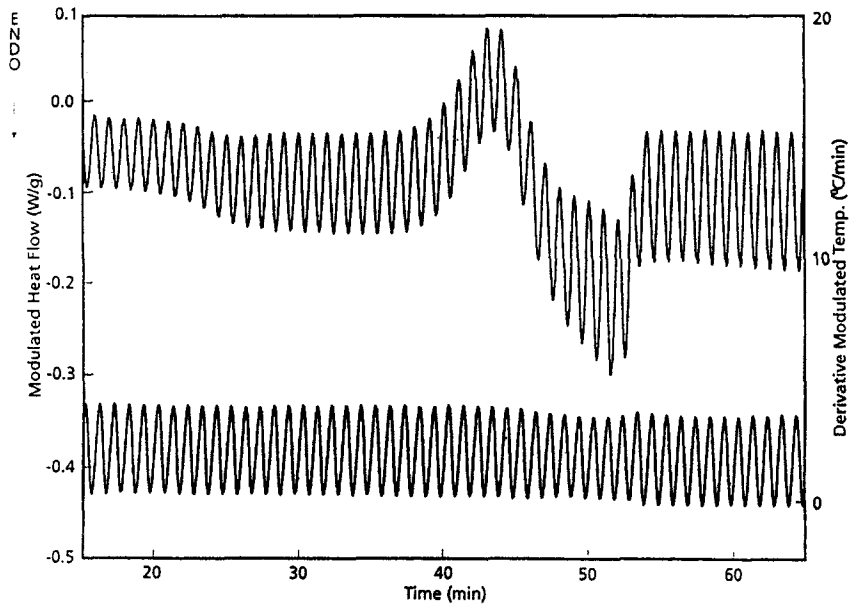

Fig. 2 The modulated heat-flow produced in response to the modulated temperature programme for a non-annealed, 65% w/w sucrose solution

Results and discussion

Non-annealed solutions

The DSC curves obtained for 20, 40 and 65% sucrose solutions are reproduced in Figs 3–5. The shapes of the total heat-flow signals (Fig. 3) were similar to those reported previously from conventional DSC at a scan rate of 5°C min^{-1} [12–15]. All the thermal events in the total heat-flow curves of this study occurred ~2°C higher than those previously reported [12–15]. The reason for this is unknown at present. The freeze-concentrated 20 and 40% sucrose solutions showed a glass transition in the reversing signals and an associated endotherm in the non-reversing curves. It can be seen that the midpoint of the step-change in the reversing signal is ~5°C higher than the step seen in the total heat-flow. This is due to the distortion of the total heat-flow caused by the enthalpic-relaxation endotherm (seen in the non-reversing signal on deconvolution).

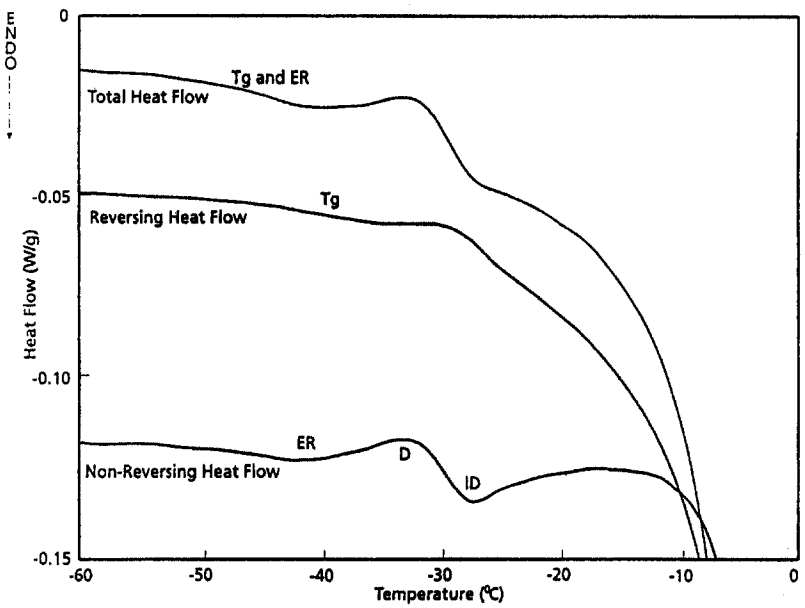

Fig. 3 Total, reversing, and non-reversing heat-flow curves obtained during the heating of a non-annealed, 20% w/w sucrose solution. T_g=glass transition, *ER*=enthalpic relaxation, *D*=devitrification and *ID*=ice dissolution

Since it is assumed that solutions had freeze-concentrated to a concentration slightly below the maximum freeze-concentration value (i.e. C_g') sucrose, a small amount of devitrification was observed in the total heat-flow curve after the glass transition. This process manifested itself as an exotherm at –35°C in the non-reversing heat-flow trace, but was not seen in the reversing heat-flow

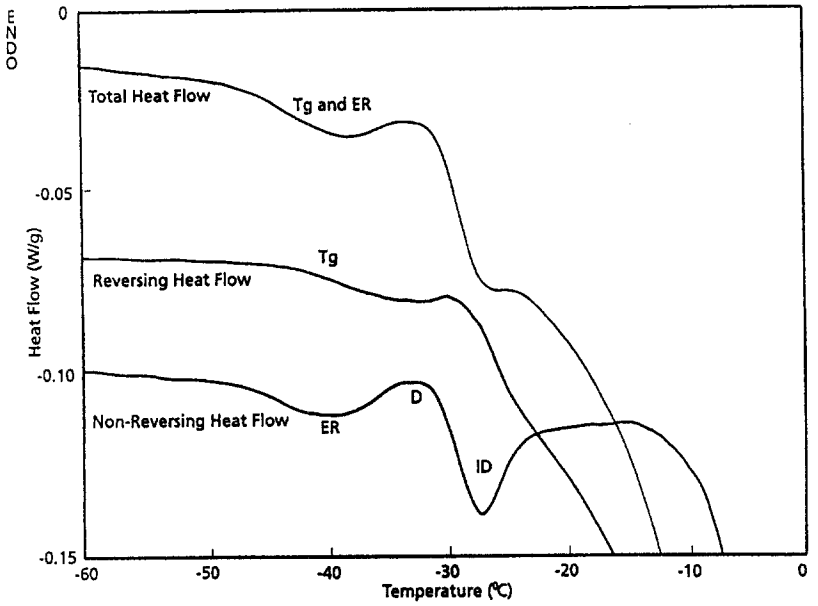

Fig. 4 Total, reversing, and non-reversing heat-flow curves obtained during the heating of a non-annealed, 40% w/w sucrose solution. T_g=glass transition, *ER*=enthalpic relaxation, *D*=devitrification and *ID*=ice dissolution

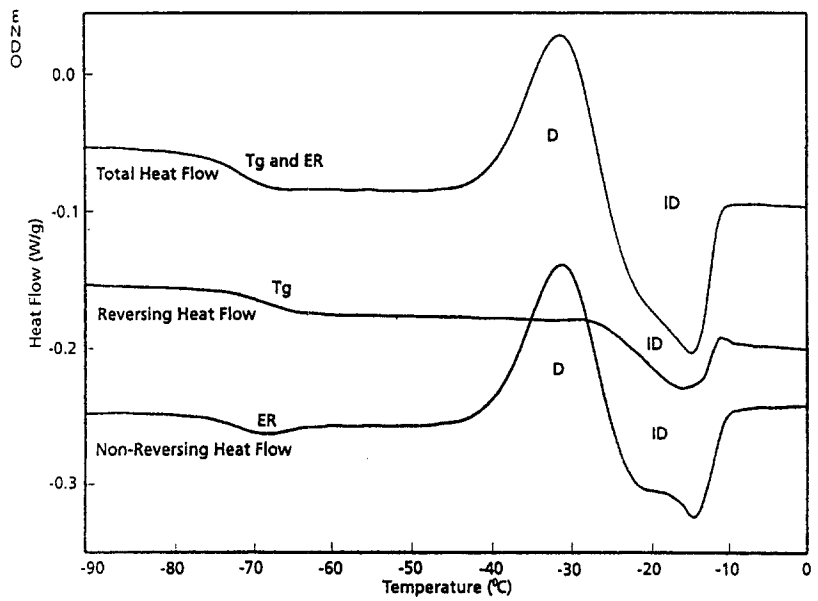

Fig. 5 Total, reversing, and non-reversing heat-flow curves obtained during the heating of a non-annealed, 65% w/w sucrose solution. T_g=glass transition, *ER* =enthalpic relaxation, *D*=devitrification and *ID*=ice dissolution

trace. An endothermic peak in the non-reversing heat-flow was also observed at about –28°C, when the ice started to dissolve into the softened glass.

The 65 % sucrose solution completely vitrified upon cooling [12], without the formation of any ice, and produced curves (Fig. 5) similar to those previously obtained for quenched polyethylene terephthalate [26]. A glass transition was observed at –75°C, where the change in heat capacity (0.49 $J\ g^{-1}\ °C^{-1}$) was similar to previously reported values [12]. The classical step-transition due to the glass transition was observed in the reversing heat-flow trace at –68°C, and this was accompanied by a relaxation endotherm in the non-reversing heat-flow curve at –70°C. A major exothermic peak occurred in the non-reversing heat-flow trace, when devitrification of ice occurred at a temperature of –40°C. This exothermic event was not observed in the reversing heat-flow trace. Dissolution of the ice at higher temperatures (–30 to 10°C) was detected in both reversing and non-reversing curves. The separation of the ice-dissolution endotherm into reversing and non-reversing curves was thought to be due to the solution being significantly perturbed from the equilibrium heat capacity *vs.* temperature profile [14] during the scan.

Annealed sucrose solutions

Glass and ice mixtures

The total heat-flow, reversing, and non-reversing DSC curves obtained for annealed solutions, with concentrations of 10–50% w/w, are shown in Figs 6–8, respectively. The total heat-flow curves (Fig. 6) were similar to those obtained previously using conventional DSC [12–14]. The T_g in the 20 and 40% solutions had increased by approximately 3°C (Fig. 6), compared to that for the non-annealed solutions (Figs 3 and 4), which is a result consistent with previous studies [20, 22] Only a minimum amount of ice devitrification was observed in these annealed samples at temperatures just above the glass transition. The sucrose solutions showed a glass transition in the reversing signal (Fig. 7) and a small associated endotherm in the non-reversing curve (Fig. 8). It can be seen that the midpoint of the step-change in the reversing signal is ~5°C higher than the step seen in the total heat flow. This is due to the distortion of the total heat flow caused by the enthalpic-relaxation endotherm (seen in the non-reversing signal (Fig. 8) on deconvolution). The thermal event, now widely but not universally regarded as corresponding to the onset of ice dissolution [8], was detected as a shoulder on the ice-melting endotherm at –30°C in the reversing curve (Fig. 7) and as a peak in the non-reversing curve (Fig. 8).

Glass only

The DSC curve obtained for an 80% w/w sucrose glass that contained no ice (Fig. 9) indicates how MDSC can be applied to resolve overlapping processes.

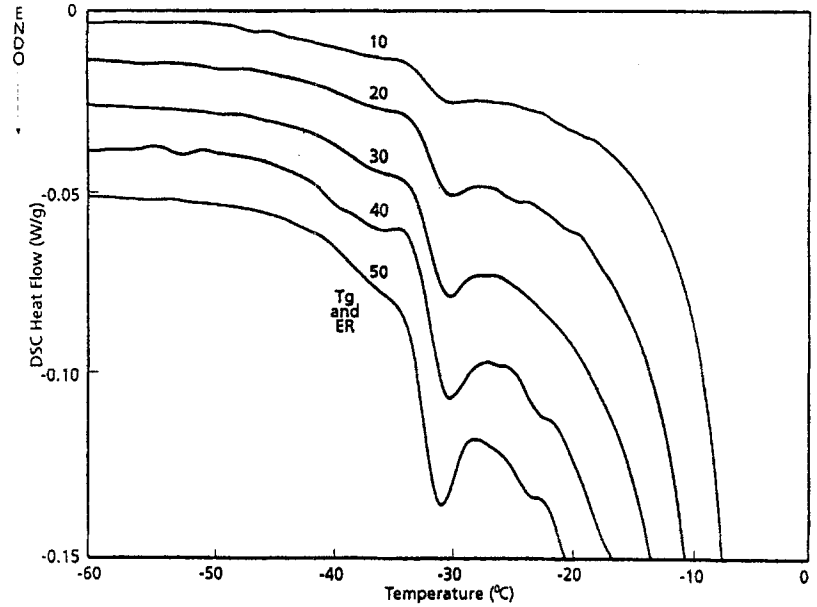

Fig. 6 Total heat-flow curves obtained on heating annealed sucrose solutions (10–50% w/w). T_g=glass transition and *ER*=enthalpic relaxation

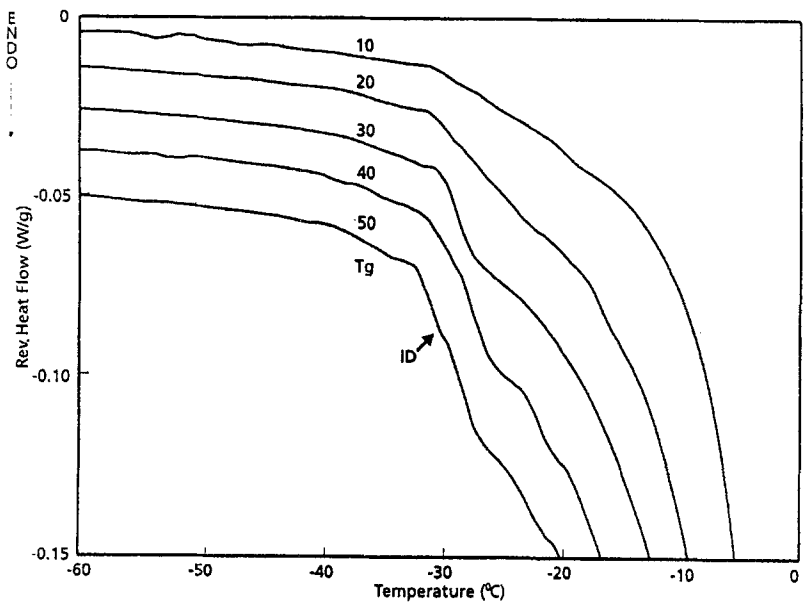

Fig. 7 Reversing heat-flow curves obtained on heating annealed sucrose solutions (10–50% w/w). T_g =glass transition and *ID*=ice dissolution

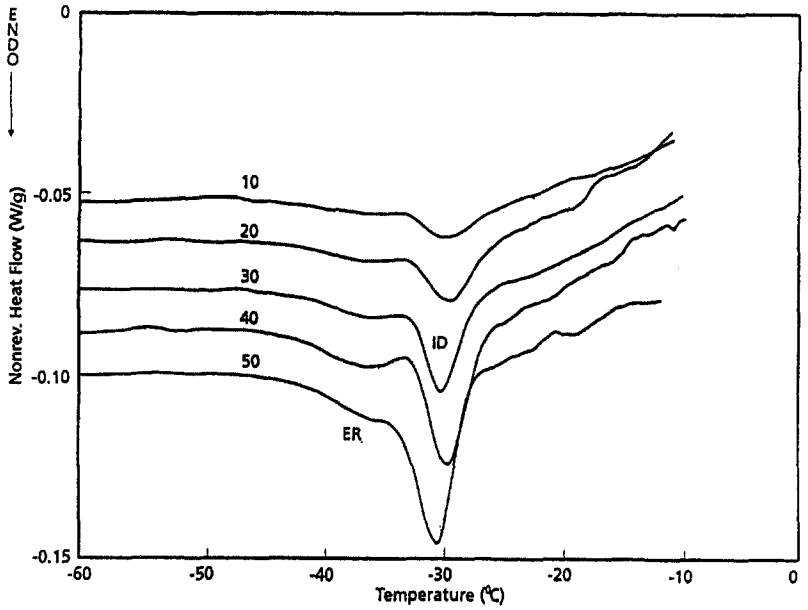

Fig. 8 Non-reversing heat-flow curves obtained on heating annealed sucrose solutions (10–50% w/w). *ER*=enthalpic relaxation and *ID*=ice dissolution

The total heat-flow curve shows the glass transition with the enthalpic relaxation superimposed upon it. The glass transition was observed as a step in the reversing signal, with an onset temperature of –38°C and a ΔC_p of 0.31 J g^{-1} $°C^{-1}$, whereas the endothermic relaxation peak was observed in the non-reversing curve, with a maximum at –31.2°C and a relaxation energy of 8.2 J g^{-1}, the latter consisting of (a) a contribution from the enthalpic relaxation that occurs at the glass transition and (b) a contribution due to the frequency dependence of the reversing signal at the glass transition.

The glass-transition event as observed in the total heat-flow signal is dependent only on the underlying (average) heating rate, whereas the glass transition as depicted in the reversing signal is dependent on both the underlying heating rate and the frequency of oscillation. The temperature of the glass-transition event is frequency-dependent and moves to higher temperature with increasing frequency. Since the frequency of the temperature oscillation (typically 10 to 100 sec per cycle) is always higher than the frequency of a "classic DSC" experiment (effectively zero) being undertaken at the same underlying heating rate, the step-change in the reversing heat-flow is always seen at a higher temperature than the step-change in the total heat flow. Since the non-reversing signal is produced by subtraction of the reversing signal from the total heat flow, the size (J g^{-1}) of the endothermic peak is influenced by the experimental con-

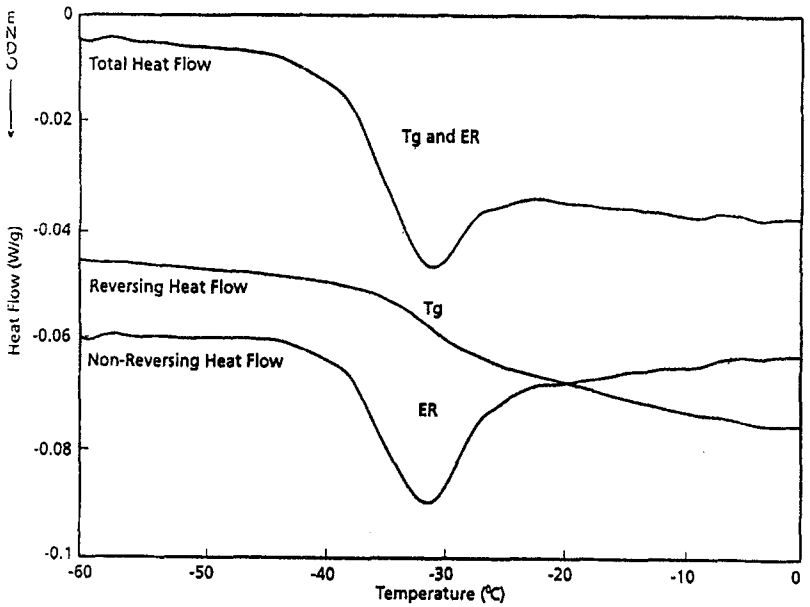

Fig. 9 Total, reversing, and non-reversing heat-flow curves obtained during the heating of an annealed, 80% w/w sucrose solution. T_g=glass transition and *ER*=enthalpic relaxation

ditions and frequency dependence of the glass transition. The contribution of frequency to the size of the peak is a constant for a given material and set of experimental conditions.

The nature of these results is similar to results obtained for an aged epoxy resin [26] and clearly demonstrates how MDSC can be used to provide new information on the characteristic features of overlapping thermal events.

Conclusions

The curves produced by MDSC on these sucrose solutions demonstrate the value of this new form of calorimetry and how it can be applied to study glass transitions in foods. Although the technique is in its infancy and the significance of the results is not yet fully understood, it is clear that MDSC has the potential to assist in providing an improved description of the thermodynamic and the kinetic processes that can take place in low- and high-moisture foods.

* * *

The authors would like to thank Mr. Mike Sahagian of the University of Guelph, Canada, for stimulating discussion during the latter stages of the preparation of this manuscript.

References

1 J. M. V. Blanshard and P. J. Lillford,eds., The Glassy State in Foods, Nottingham University Press, Loughborough 1993.
2 P. Fito, A. Mulet and B. McKenna, eds., Water in Foods, Elsevier Applied Science, London 1994.
3 H. Levine and L. Slade, Cryo-Lett., 9 (1988) 21.
4 L. Slade and H. Levine, Crit. Rev. Food Sci. Nutr., 30 (1991) 115.
5 Y. H. Roos, Phase Transitions in Foods, Academic Press, London 1995.
6 Water activity: A credible measure of technological performance and physiological viability?, Royal Society of Chemistry Conference, Girton College, Cambridge, UK, 1–3 July, 1985.
7 Y. Roos and M. Karel, Food Technol., 45 (12) (1991) 66, 68, 107.
8 Proc. of Amorphous Carbohydrates: Chemistry and Application Technology Workshop, Girton College, Cambridge, UK 1995.
9 D. S. Reid, J. Hsu and W. Kerr, in The Glassy State in Foods, eds. J. M. V. Blanshard and P. J. Lillford, Nottingham University Press, Loughborough 1993, p. 123.
10 D. Simatos and G. Blond, in Water Relationships in Foods, Plenum, New York 1991, p. 139.
11 M. E. Sahagian and H. D. Goff, Food Res. Int., 28 (1995) 1.
12 M. J. Izzard, S. Ablett and P. J. Lillford, Food Polymers, Gels and Colloids (ed. E. Dickenson), Royal Society of Chemistry, Cambridge 1991, p. 289.
13 S. Ablett, M. J. Izzard and P. J. Lillford, J. Chem. Soc. Faraday Trans., 88 (1992) 789.
14 S. Ablett, A. Clark, M. J. Izzard and P. J. Lillford, J. Chem. Soc. Faraday Trans., 88 (1992) 795.
15 Y. Roos and M. Karel, Int. J. Food Sci. Technol., 26 (1991) 553.
16 D. Simatos and G. Blond, in The Glassy State in Foods, eds. J. M. V. Blanshard and P. J. Lillford, Nottingham University Press, Loughborough 1993, p. 395.
17 Y. Roos and M. Karel, J. Food Sci., 55 (1991) 266.
18 M. Reading, D. Elliott and V. Hill, Proc. 2lst NATAS Conf. 1992 p. 145.
19 R. Sauerbrunn, B.S. Crowe and M. Reading, Proc. 2lst NATAS Conf., 1992 p. 137.
20 S. R. Sauerbrunn, B. S. Crowe and M. Reading, Amer. Lab., 24 (1992) 44.
21 B. Wunderlich, Y. Lin and A. Boller, Thermochim. Acta, 238 (1994) 277.
22 M. Reading, Trends Polym. Sci., 1 (1993) 248.
23 A. Boller, C. Schick and B. Wunderlich, Thermochim. Acta, 266 (1995) 97.
24 N. Buckman, Chem. Australia, Dec. (1993) 666.
25 M. Reading, B. K. Hahn and B. S. Crowe, U. S. Patent 5, 224, 775 (1993).
26 M. Reading TRIP, 1 (1993) 248.
27 H. D. Goff and M. E. Sahagian, Thermochim. Acta, in press.
28 H. D. Goff, Pure Appl. Chem., 67 (1995) 1801.
29 J. L. McNaughton and C. T. Mortimer, Differential Scanning Calorimetry, IRS, Physical Chemistry Series 2, Butterworths, London 1975, p. 10.